

Prediction of Room-Temperature Superconductivity in Quasi-atomic H₂-Type Hydrides at High Pressure

Qiwen Jiang^a, Defang Duan^{a,*}, Hao Song^b, Zihan Zhang^a, Zihao Huo^a, Shuqing

Jiang^{c,a}, Tian Cui^{b,a,*}, Yansun Yao^d

^a Key Laboratory of Material Simulation Methods & Software of Ministry of Education and State Key Laboratory of Superhard Materials, College of Physics, Jilin University, Changchun 130012, China

^b Institute of High Pressure Physics, School of Physical Science and Technology, Ningbo University, Ningbo, 315211, China

^c Synergetic Extreme Condition User Facility, College of Physics, Jilin University, Changchun, Jilin 130012, China

^d Department of Physics and Engineering Physics, University of Saskatchewan, Saskatoon, Saskatchewan S7N 5E2, Canada

* Corresponding author: duandf@jlu.edu.cn (Defang Duan), cuitian@nbu.edu.cn (Tian Cui)

Abstract

Achieving superconductivity at room temperature (RT) is a holy grail in physics. Recent discoveries on high- T_c superconductivity in binary hydrides H_3S and LaH_{10} at high pressure have directed the search for RT superconductors to compress hydrides with conventional electron-phonon mechanisms. Here, we predict an exceptional family of superhydrides under high pressures, $M\text{H}_{12}$ ($M = \text{Mg}, \text{Sc}, \text{Zr}, \text{Hf}, \text{Lu}$), all exhibiting RT superconductivity with calculated T_c s ranging from 313 to 398 K. In contrast to H_3S and LaH_{10} , the hydrogen sublattice in $M\text{H}_{12}$ is arranged as quasi-atomic H_2 units. This unique configuration is closely associated with high T_c , attributed to the high electronic density of states derived from H_2 antibonding states at the Fermi level and the strong electron-phonon coupling related to the bending vibration of H_2 and H- M -H. Notably, MgH_{12} and ScH_{12} remain dynamically stable even at pressure below 100 GPa. Our findings offer crucial insights into achieving RT superconductivity and pave the way for innovative directions in experimental research.

It was predicted that solid hydrogen would become metallic in the atomic state under extreme compression [1]. Theoretically, metallic hydrogen has all the ingredients needed for a room-temperature (RT) superconductor, *e.g.*, high-frequency phonons, high density of states (DOS) at the Fermi level, and very strong electron-phonon coupling (EPC) [2]. However, the direct compression of solid hydrogen may require pressure over 500 GPa [3-5] to reach a metallic state, which poses extreme difficulty in experiments. Alternatively, in compressed hydrides, the hydrogen species are ‘precompressed’ [6] by the metal elements, and therefore, the charge density sufficient for metallization can be achieved at less physical compression [7-10]. Currently, all experimentally synthesized high- T_c hydrides necessitate high pressures above 150 GPa, but T_c below RT [11-19]. The primary goal in physics and material science is to achieve RT superconductivity at pressures below 100 GPa, ultimately reaching ambient pressure conditions.

Diatomic H_2 is a ubiquitous building block of solid hydrogen (*e.g.*, phase I, II, III [20-22]) and of many hydrides as well [7], such as theoretically predicted $SiH_4(H_2)_2$ [23] and TeH_4 [24], and experimentally synthesized BaH_{12} [25], SrH_{22} [26], HfH_{14} [27], and SnH_{12} [28], *etc.* These ‘molecular’ hydrides usually exhibit moderate superconductivity with a T_c below 120 K since the hydrogen electrons occupy bonding orbitals far below the Fermi level, resulting in a low DOS, even an insulating state. Breaking H_2 molecular units is a prerequisite for achieving high- T_c superconductivity [29-32]. To increase the T_c in hydrides, one needs to ‘free’ electrons from their locked positions, that is, to weaken the H_2 units toward atomic hydrogen. This will allow the H electrons to occupy energy states closer to the Fermi level. Two prototypic hydrides consisting of atomic hydrogen sublattices, the cubic H_3S [11,12,33,34] and cage-like LaH_{10} [13-15,30,35,36], were predicted following this principle and subsequently confirmed by experiments. These two hydrides have very high measured T_c s in the 200-260 K range. Thus, the high- T_c hydrides are recognized as being associated with weakened H_2 units.

In the present work, we have predicted a novel group of dodecahydrides, MH_{12} ($M =$

Mg, Sc, Zr, Hf, Lu), calculated to have T_c values exceeding RT. Different from previously reported atomic (H_3S), cage (LaH_{10}), and planar (HfH_{10} [37]) forms, hydrogen atoms in MH_{12} are regularly arranged in quasi-atomic peanut-like H_2 units. All dodecahydrides in this study are predicted to be RT superconductors with T_c up to 313-398 K estimated by solving Eliashberg equations. In particular, ScH_{12} and MgH_{12} are the first RT hydride superconductors hitherto predicted to exist at pressures below 100 GPa. Adding one H atom into the MH_{12} , we obtained a class of MH_{13} containing quasi-molecular H_2 units, which also exhibit high T_c s but are notably lower than their respective MH_{12} counterparts. Our research provides a promising approach for investigating phonon-mediated RT superconductivity at lower pressures that meet or surpass the atomic metallic hydrogen.

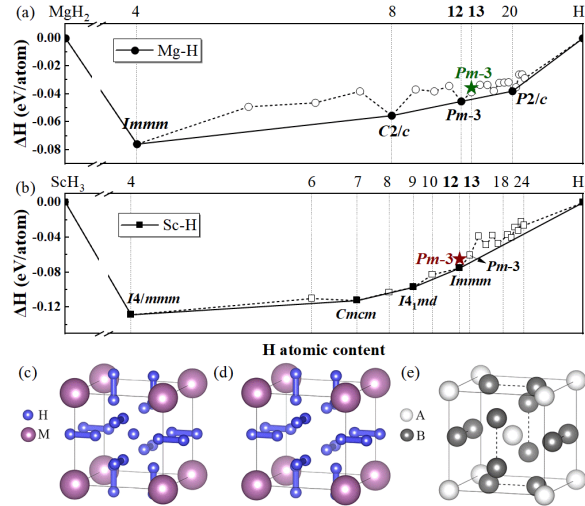


Fig. 1. The thermodynamic convex hull diagram of (a) Mg-H and (b) Sc-H systems at 300 GPa with ZPE included. The red and green stars near the convex hull correspond to the $Pm\bar{3}$ - ScH_{12} and $Pm\bar{3}$ - MgH_{13} phases, respectively. Crystal structure of (c) MH_{13} , (d) MH_{12} , and (e) the $A15$ type structure (AB_3 , $Pm\bar{3}n$).

Recently reported high- T_c hydrides mainly have the metal elements in the 2nd and 3rd groups of the periodic table [38]. Mg and Sc represent the lightest elements among them (except for Be) and serve as the primary focus of our study. We performed variable composition structural searches for Mg-H and Sc-H systems at 200 and 300 GPa using

AIRSS code [39]. The convex hull diagram in Fig. 1 illustrates the formation enthalpies for the optimal structures in all studied Mg-H and Sc-H stoichiometries. Zero-point energy (ZPE) was included in the enthalpy calculation to account for the quantum effects. In this search, we successfully recovered the previously predicted structures from Refs. [40-42]. Moreover, two unique hydrides, MH_{12} and MH_{13} ($M = \text{Mg}$ and Sc), with distinct $Pm\bar{3}$ symmetry, appeal to our attention. Both at 200 GPa and 300 GPa, MgH_{12} and ScH_{12} lies on the convex hull, while ScH_{13} and MgH_{13} slightly surpass the hull by about ~ 8 meV/atom, as shown in Fig. 1 and Fig. S1 of supplementary material (SM). Due to synthesizing hydrides typically involving laser heating [18,19,43-45], we considered the temperature effect through quasi-harmonic free energy calculations (Fig. S2). We found that the $Pm\bar{3}$ phase of MgH_{12} is more stable than the $R\bar{3}$ phase at above 200 GPa and 1400 K, while the $Pm\bar{3}$ phase of ScH_{12} becomes more stable than the ground state $P6_4$ and $Immm$ at temperatures above 1700 K within the range of 200-400 GPa. These results suggest the synthesis potential of ScH_{12} and MgH_{12} within the pressure range of 200-300 GPa, alongside high temperatures.

To examine the dynamical stability of MH_{12} and MH_{13} ($M = \text{Mg}$ and Sc), we calculated their phonon spectra at different pressures (Figs. S21-24). There are no imaginary phonon frequencies for MgH_{12} at 210 GPa and above, and for MgH_{13} at 300 GPa and above, which establish their dynamic stability ranges. ScH_{12} and ScH_{13} are dynamically stable down to a low pressure of 90 GPa. We extended the investigation to other isostructural MH_{12} and MH_{13} compounds involving other metal elements and identified Zr, Hf, and Lu, guided by criteria of similar Pauling electronegativity (~ 1.3) and atomic radius (~ 1.6 Å). Subsequent phonon dispersion relation calculations confirm that these three metals' corresponding MH_{12} and MH_{13} are dynamically stable (Fig. S22-24). In comparison, MH_{12} and MH_{13} hydrides with Ca, Y, La, Ac and Th are dynamically unstable up to 600 GPa due to large atomic radius or low electronegativity (Fig. S6).

In the $Pm\bar{3}$ - MH_{13} , M atoms form a cubic lattice with a single H atom occupying the center. A pair of H_2 units are perpendicular to and intersecting each face of the cube

(Fig. 1c). If the centred H atom is removed, the structure will turn into the $Pm\bar{3}$ - MH_{12} structure (Fig. 1d). The structures of MH_{12} and MH_{13} are viewed as variants of the $A15$ type (AB_3 , $Pm\bar{3}n$), with M and diatomic H_2 being the two bases (see Fig. 1e). The structural information is listed in the Table S1. Interestingly, the $A15$ structure has been known to exist in conventional superconductors, such as Nb_3Sn and Nb_3Ge [46]. There are also $A15$ -type superconductors in metal hydrides. For example, GaH_3 and GeH_3 have high T_c of 123 K at 120 GPa [46] and 140 K at 180 GPa [47], respectively. Ternary hydride $LiPH_6$ [48] also adopts the $A15$ -like configuration, which is predicted to be a high- T_c superconductor (150-167 K at 200 GPa).

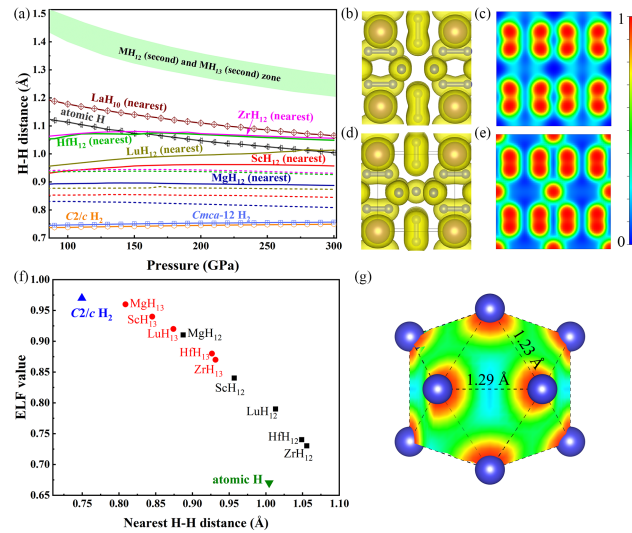


Fig. 2. (a) Distance between H atoms in MH_{12} (solid lines) and MH_{13} (dashed lines of the same color) compared to atomic and molecular hydrogen as a function of pressure. 3D ELF of (b) ScH_{12} and (d) ScH_{13} with isosurface value of 0.6. 2D ELF of (c) ScH_{12} and (e) ScH_{13} for the (0 0 2) plane at 300 GPa. (f) The ELF value varies with the nearest H-H distance of $MH_{12,13}$, molecular H_2 and atomic H at 300 GPa. (g) ELF cut plane of hydrogen icosahedron of ScH_{12} at 300 GPa.

The bonding characteristics of MH_{12} and MH_{13} are investigated using electron localization function (ELF), crystal orbital Hamiltonian population (COHP), and Bader charge analysis. Bader analysis (Table S2) reveals significant charge transfer from the M atom to the H atoms, while each H_2 pair receives more electrons in MH_{12} than in

MH_{13} . $ScH_{12,13}$ serves as a typical example at 300 GPa. In ScH_{12} , each H_2 pair accepts $0.190 e^-$, while each H_2 pair accepts $0.164 e^-$ in ScH_{13} . Since the electrons acquired by hydrogen must populate their antibonding states, this weakens the H-H bonds. In Fig. 2a, we compare the nearest and the second nearest H-H distances of MH_{12} and MH_{13} to those in atomic H ($I4_1/amd$) and molecular H_2 solids ($C2/c$ and $Cmca-12$ phases). H-H contacts in both MH_{12} and MH_{13} are longer than the covalent bond length in molecular H_2 , as one would expect for weakened bonds. On average, shorter H-H bonds in MH_{13} than in MH_{12} are consistent with fewer electrons in the antibonding orbitals. Interestingly, similar to molecular H_2 , the H-H contact in MH_{13} does not change with pressure, indicating that the latter still contains molecular H_2 , albeit weaker in strength. We thus term the H_2 units in MH_{13} as ‘quasi molecular’. On the other hand, the H-H bond length in MH_{12} keeps increasing at higher pressures, showing a pronounced tendency for H_2 molecule dissociation, and reaches almost the same value as that in atomic hydrogen at 300 GPa. The important molecular feature of H_2 molecular stretching vibrational modes near the frequency of 3000 cm^{-1} is absent in MH_{12} (see Fig. S21-22). Hence, it seems reasonable to refer to the H_2 unit in MH_{12} as ‘quasi atomic’. The electron clouds surrounding quasi-atomic H_2 are shaped like peanuts, with a high ELF value of ~ 0.84 for ScH_{12} (Fig. 2b-2c and Figs. S6-S9). Additionally, the ELF value between adjacent H_2 units (perpendicular) at a distance of 1.23 \AA is approximately 0.45, exhibiting metallic interaction with free electrons connectivity (Fig. 2g). As shown in Fig. 2f, the H-H bonds in MH_{12} and MH_{13} display distinct electron localization characteristics, with the ELF values showing an approximately linear correlation with the H-H bond lengths. The calculated integrated crystalline orbital Hamiltonian population (ICOHP) values within the H_2 units (Figs. S11-12) are -3.23 eV in ScH_{12} and -4.91 eV in ScH_{13} , indicating a much stronger bonding interaction in the latter. The ICOHP values between the H_2 units (perpendicular) are -0.91 eV in ScH_{12} and -0.55 eV in ScH_{13} . This manifests a weak inter-molecular interaction in ScH_{12} , which causes the weakening of the H_2 units.

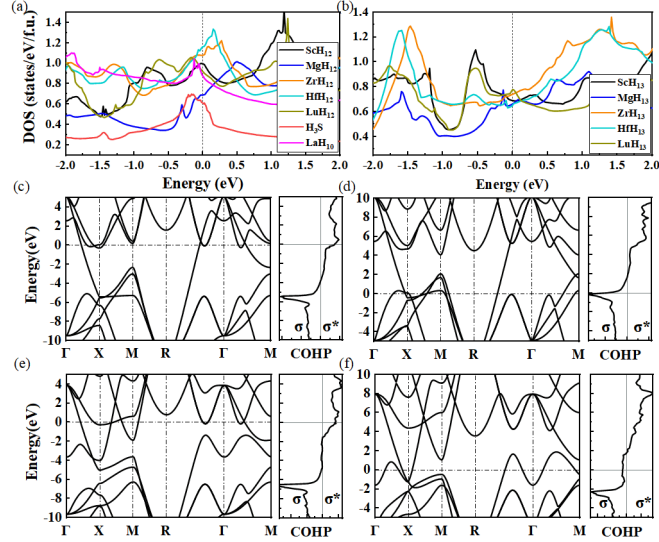


Fig. 3. Total DOS of (a) MH_{12} and (b) MH_{13} compared to H_3S and LaH_{10} . Electronic band structures and COHP of H-H bonds for (c) MgH_{12} , (d) Mg_0H_{12} , (e) MgH_{13} , and (f) Mg_0H_{13} at 300 GPa.

The electronic band structures and project DOS of MH_{12} and MH_{13} are shown in Fig. 3 and Figs. S27-S31. Given the uniqueness of magnesium superhydrides, we first discuss other $XH_{12, 13}$ ($X = Sc, Zr, Hf, Lu$). A common feature displayed in these XH_{12} is the van Hove singularity with a large total DOS value at the Fermi level (Fig. 3a), formed by strong hybridization of d -orbital (f -orbital) of metal atoms and the s -orbital of H atoms (Figs. S28-S31). In contrast, the DOS in XH_{13} is notably uniform around the Fermi level (Fig. 3b). The van Hove singularity plays an important role in enhancing the EPC and increasing T_c in H_3S and LaH_{10} . The comparison of XH_{12} to H_3S and LaH_{10} at 300 GPa shows that XH_{12} has a significantly larger DOS at the Fermi level, with a trend of $XH_{12} > LaH_{10} > XH_{13} > H_3S$ (Fig. 3a). High electronic DOS at the Fermi level, in particular those induced by hydrogen, sets a favourable condition for Cooper pairs, strong EPC and superconductivity. The electronic structures of MgH_{12} and MgH_{13} are different from $XH_{12, 13}$, characterized by nearly unoccupied d -states of Mg in the valence bands, and H atoms significantly contribute to the total DOS ($\sim 86\%$). As shown in Figs. 3c-3f, the band structures of MgH_{12} and MgH_{13} highly resemble Mg_0H_{12} and Mg_0H_{13} (hypothetical structures with Mg removed from the hydrides, without relaxation),

exhibiting a pure hydrogen character. The presence of Mg provides electrons to the H₂ units, which elevate the Fermi level from the low-energy bonding states (σ) to the antibonding states (σ^*), maximizing the electronic states of H at the Fermi level. We observe interlocking electron pockets near the X point, especially in MgH₁₂, where the nearly degenerate A_g and A_u bands at the X point and the hole pocket at the Γ point, create a fish-tail-shaped Fermi surface along the Γ -X direction (Fig. S30). The subsequent peak of the nesting function $\xi(Q)$ in that direction indicates strong Fermi surface nesting, which is advantageous for EPC (Fig. S31).

To examine the superconducting properties of $MH_{12,13}$, we calculated the logarithmic average phonon frequency (ω_{\log}), EPC parameter (λ), and Eliashberg phonon spectral function [$\alpha^2F(\omega)$] (Figs. S21-23). It should be noted that the vibrational bands of hydrogen in MgH₁₂ and ScH₁₂ hydrides are mixed and dispersive, with all frequencies below 2800 cm⁻¹ (Fig. S21) at 300 GPa, consistent with the disappearance of molecular H₂. For MgH₁₃ and ScH₁₃, the high-frequency vibrations still form an isolated non-dispersive block, peaking at approximately 3000 cm⁻¹. This frequency aligns with the stretching vibrations of quasi-molecular H₂, yet their contribution to the EPC is minor (< 10%). For pure molecular hydrogen $C2/c$ and $Cmca-12$ phases [49], the highest vibrational frequency is around 4000 cm⁻¹ at 250 GPa. The lower hydride vibrational frequencies indicate weaker H-H bonds induced by the interaction between H and metal atoms. Compared to MH_{13} , the calculated λ values for all MH_{12} compounds within their dynamically stable pressure range are greater than or equal to 2.5, suggesting a very strong EPC. The remarkable λ values are mainly associated with mixed stretching, rocking and scissoring vibrations of the H₂ units within the mid-frequency range, accompanied by the bending vibrations of H-Sc-H (Fig. S25). Using typical Coulomb pseudopotential $\mu^* = 0.1-0.13$, applying the Eliashberg equations yields a very high T_c value ranging 304-325 K for ScH₁₂ with $\lambda = 2.50$ at 300 GPa (Table S3). In the case of ScH₁₃, the highest T_c is calculated to be 185 K ($\mu^* = 0.1$) with $\lambda = 1.40$, much lower than that of ScH₁₂. MgH₁₂ and MgH₁₃ exhibit RT superconductivity, with T_c values of 366-388 K and 303-324 K at 300 GPa, respectively. MH_{12} ($M=Zr, Hf, \text{ and Lu}$) are also

calculated to have RT T_c between 333 K and 388 K, and MH_{13} hosts high T_c with 160-200 K ($\mu^* = 0.10$).

As shown in Fig. 4a, the superhydrides MH_{12} investigated in this study exhibit remarkably high T_c values comparable to atomic metallic hydrogen (~ 356 K at 500 GPa [50]), particularly with substantially reduced stability pressures in Sc and Mg. This highlights the potential of MH_{12} superhydrides as promising candidates for RT superconductors. Strikingly, the superconductivity of ScH_{12} shows weak dependence on pressure, maintaining RT superconductivity down to a significantly lower pressure of 90 GPa when compared to other compressed hydrides (e.g., YH_{10} and Li_2MgH_{16} at 250 GPa).

Given the light mass of hydrogen, anharmonicity is crucial for superhydrides, especially those with strong EPC [51,52]. Due to the substantial computational cost, we take MgH_{12} as an example and examined this effect using the stochastic self-consistent harmonic approximation [53]. As shown in Fig. S26, the anharmonic correction hardens phonon modes near the Γ -point, eliminating instability above 70 GPa. At 210 GPa, the anharmonicity weakens the EPC parameter while enhancing \log , resulting T_c slightly decreases to 345-365 K (Table S1), maintaining above RT. At 70 GPa, the anharmonic T_c value is 281-296 K, still close to RT.

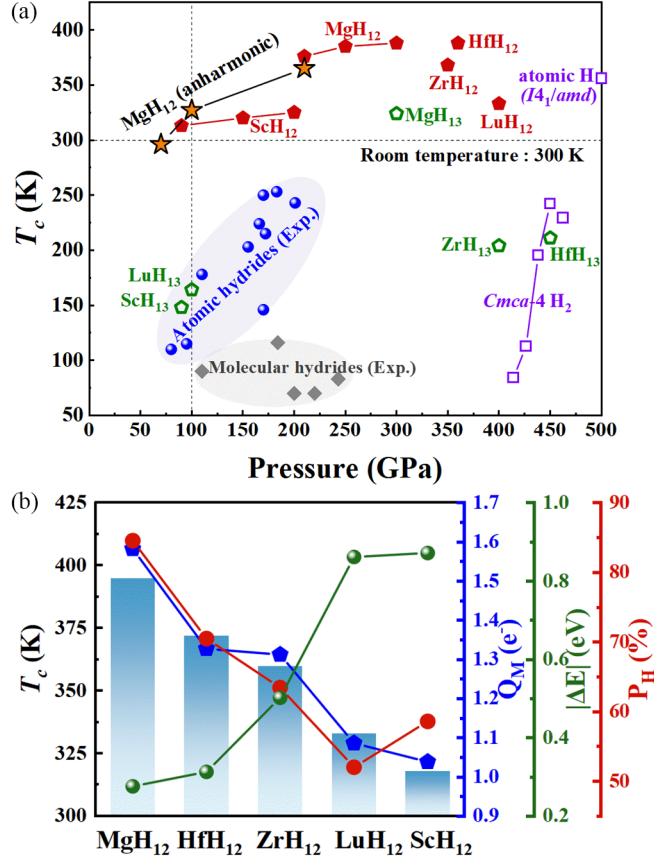


Fig. 4. (a) Calculated T_c of MH_{12} and MH_{13} by numerically solving Eliashberg equations at different pressures with $\mu^* = 0.10$. The blue circles and gray squares denote the well-known hydrides from experiments [11-19,27,28,44,45,54-60]. Superconductivity in molecular hydrogen ($Cmca-4$) and atomic hydrogen ($I4_1/amd$) is documented in Ref. [50,61]. (b) Calculated at 400 GPa for MH_{12} , the T_c , the electrons transferred from M to hydrogen atoms (Q_M), the percentage of the H electronic DOS at the Fermi level (P_H), and the distance between the H-H antibonding state and the Fermi level at the X point ($|\Delta E|$).

As discussed above, the intriguing RT superconductivity of MH_{12} is related to the transferred electrons from metal M to H atoms (Q_M), the percentage of H electronic DOS (P_H), and the energy difference ($|\Delta E|$) between the flat band at the X point and the Fermi level (Fig. S34). To gain further insights, we plotted the relationship between these parameters and T_c , as shown in Fig. 4b. From Sc to Lu, Zr, Hf, and finally to Mg, there is an increasing electron transfer from metals to hydrogen, elevating the Fermi energy and leading to a decrease in $|\Delta E|$. This brings the antibonding orbitals of

hydrogen corresponding to the flat band closer to the Fermi level, maximizing the DOS contribution of hydrogen and promoting the formation of Cooper pairs. Consequently, the EPC constant for the optical modes derived from hydrogen at the X point gradually strengthens (Fig. S35), increasing T_c .

In previous research, it was thought that hydrides containing H_2 or H_3 molecular units are unfavorable for superconductivity. However, this study found a particular case, MgH_{13} , with quasi-molecular H_2 units exhibiting RT superconductivity. As shown in Fig. S36, the H-H bond length does not display a singular linear relationship with T_c . Hence, inferring T_c based solely on this criterion appears to be rudimentary. We further performed a statistical analysis of the relationship between T_c and the product of P_H and the DOS per hydrogen atom ($DOS_{\text{per H}}$), and the results show a positive correlation (Fig. S37). It is necessary to calculate the DOS of hydrogen at the Fermi level to predict the possibility of hydride superconductivity [62]. The pure hydrogen framework of H_{12} offers a plethora of unoccupied energy levels. In certain s/p block metal hydrides like Mg, extra electrons support the prominent DOS associated with the dominant antibonding states of H_2 , albeit with a minor inclination towards molecular dissociation.

In summary, an extensive structure search combined with *ab initio* calculations reveals a unique superhydride MH_{12} ($M = Mg, Sc, Zr, Hf, Lu$) under high pressure. In this structure, hydrogen atoms are arranged in quasi-atomic peanut-like H_2 units, which differs significantly from the hydrogen configurations in known high- T_c hydrides H_3S and LaH_{10} . MH_{12} is calculated to have a superconducting critical temperature T_c similar to or superior to metallic hydrogen solids, exhibiting superconductivity at the highest temperature among all known/predicted binary hydrides. In MH_{13} , hydrogen atoms form quasi-molecular H_2 units, which are also predicted to possess high T_c . The intriguing family of RT superconducting hydrides we have predicted is poised to stimulate future high-pressure experimental investigations, potentially enabling synthesis within diamond anvil cells through laser heating.

Acknowledgements

This work was supported by the National Key Research and Development Program of China (No. 2022YFA1402304), the National Natural Science Foundation of China (Grants No. 12122405, No. 52072188, No. 12274169, and No. 51632002), the Natural Sciences and Engineering Research Council of Canada (NSERC), program for Science and Technology Innovation Team in Zhejiang (No. 2021R01004) and the Fundamental Research Funds for the Central Universities. Some calculations were performed at the High Performance Computing Center of Jilin University and using TianHe-1(A) at the National Supercomputer Center in Tianjin.

Competing interests

The authors declare no competing interests.

References

- [1] E. WIGNER and B. H. HUNTINGTON, *On the possibility of a metallic modification of hydrogen*, J Chem Phys **3**, 764, (1935).
- [2] N. W. Ashcroft, *Metallic Hydrogen: A High-Temperature Superconductor?*, Physical Review Letters **21**, 1748, (1968).
- [3] P. Loubeyre, F. Occelli, and P. Dumas, *Synchrotron infrared spectroscopic evidence of the probable transition to metal hydrogen*, Nature **577**, 631, (2020).
- [4] J. McMinis, R. C. Clay, D. Lee, and M. A. Morales, *Molecular to atomic phase transition in hydrogen under high pressure*, Phys Rev Lett **114**, 105305, (2015).
- [5] M. I. Eremets, A. P. Drozdov, P. P. Kong, and H. Wang, *Semimetallic molecular hydrogen at pressure above 350 GPa*, Nature Physics **15**, 1246, (2019).
- [6] N. W. Ashcroft, *Hydrogen dominant metallic alloys: high temperature superconductors?*, Phys Rev Lett **92**, 187002, (2004).
- [7] D. Duan, Y. Liu, Y. Ma, Z. Shao, B. Liu, and T. Cui, *Structure and superconductivity of hydrides at high pressures*, National Science Review **4**, 121, (2017).
- [8] J. A. Flores-Livas, L. Boeri, A. Sanna, G. Profeta, R. Arita, and M. Eremets, *A perspective on conventional high-temperature superconductors at high pressure: Methods and materials*, Physics Reports **856**, 1, (2020).
- [9] G. Gao, L. Wang, M. Li, J. Zhang, R. T. Howie, E. Gregoryanz, V. V. Struzhkin, L. Wang, and J. S. Tse, *Superconducting binary hydrides: Theoretical predictions and experimental progresses*, Materials Today Physics **21**, (2021).
- [10] M. Du, W. Zhao, T. Cui, and D. Duan, *Compressed superhydrides: the road to room temperature superconductivity*, J Phys Condens Matter **34**, (2022).
- [11] A. P. Drozdov, M. I. Eremets, I. A. Troyan, V. Ksenofontov, and S. I. Shylin, *Conventional superconductivity at 203 kelvin at high pressures in the sulfur hydride system*, Nature **525**, 73, (2015).
- [12] M. Einaga, M. Sakata, T. Ishikawa, K. Shimizu, M. I. Eremets, A. P. Drozdov, I. A. Troyan, N. Hirao, and Y. Ohishi, *Crystal Structure of the Superconducting Phase of Sulfur Hydride*, Nat Phys **12**, 835, (2016).
- [13] Z. M. Geballe, H. Liu, A. K. Mishra, M. Ahart, M. Somayazulu, Y. Meng, M. Baldini, and R. J. Hemley, *Synthesis and Stability of Lanthanum Superhydrides*, Angew Chem Int Ed Engl **57**, 688, (2018).
- [14] A. P. Drozdov, P. P. Kong, V. S. Minkov, S. P. Besedin, M. A. Kuzovnikov, S. Mozaffari, L. Balicas, F. F. Balakirev, D. E. Graf, V. B. Prakapenka, E. Greenberg, D. A. Knyazev, M. Tkacz, and M. I. Eremets, *Superconductivity at 250 K in lanthanum hydride under high pressures*, Nature **569**, 528, (2019).
- [15] M. Somayazulu, M. Ahart, A. K. Mishra, Z. M. Geballe, M. Baldini, Y. Meng, V. V. Struzhkin, and R. J. Hemley, *Evidence for Superconductivity above 260 K in Lanthanum Superhydride at Megabar Pressures*, Phys Rev Lett **122**, 027001, (2019).
- [16] I. A. Troyan, D. V. Semenov, A. G. Kvashnin, A. V. Sadakov, O. A. Sobolevskiy, V. M. Pudalov, A. G. Ivanova, V. B. Prakapenka, E. Greenberg, A. G. Gavriluk, I. S. Lyubutin, V. V. Struzhkin, A. Bergara, I. Errea, R. Bianco, M. Calandra, F. Mauri, L. Monacelli, R. Akashi, and A. R. Oganov, *Anomalous High-Temperature Superconductivity in YH₆*, Adv Mater, e2006832, (2021).
- [17] P. Kong, V. S. Minkov, M. A. Kuzovnikov, A. P. Drozdov, S. P. Besedin, S. Mozaffari, L. Balicas, F. F. Balakirev, V. B. Prakapenka, S. Chariton, D. A. Knyazev, E. Greenberg, and M. I. Eremets, *Superconductivity up to 243 K in the yttrium-hydrogen system under high pressure*, Nat Commun **12**, 5075, (2021).

- [18] Z. Li, X. He, C. Zhang, X. Wang, S. Zhang, Y. Jia, S. Feng, K. Lu, J. Zhao, J. Zhang, B. Min, Y. Long, R. Yu, L. Wang, M. Ye, Z. Zhang, V. Prakapenka, S. Chariton, P. A. Ginsberg, J. Bass, S. Yuan, H. Liu, and C. Jin, *Superconductivity above 200 K discovered in superhydrides of calcium*, Nature Communications **13**, (2022).
- [19] L. Ma, K. Wang, Y. Xie, X. Yang, Y. Wang, M. Zhou, H. Liu, X. Yu, Y. Zhao, H. Wang, G. Liu, and Y. Ma, *High-Temperature Superconducting Phase in Clathrate Calcium Hydride CaH₆ up to 215 K at a Pressure of 172 GPa*, Phys Rev Lett **128**, 167001, (2022).
- [20] C. J. Pickard and R. J. Needs, *Structure of phase III of solid hydrogen*, Nature Physics **3**, 473, (2007).
- [21] P. Loubeyre, R. LeToullec, D. Hausermann, M. Hanfland, R. J. Hemley, H. K. Mao, and L. W. Finger, *X-ray diffraction and equation of state of hydrogen at megabar pressures*, Nature **383**, 702, (1996).
- [22] H.-k. Mao and R. J. Hemley, *Ultrahigh-pressure transitions in solid hydrogen*, Reviews of Modern Physics **66**, 671, (1994).
- [23] Y. Li, G. Gao, Y. Xie, Y. Ma, T. Cui, and G. Zou, *Superconductivity at approximately 100 K in dense SiH₄(H₂)₂ predicted by first principles*, Proc Natl Acad Sci U S A **107**, 15708, (2010).
- [24] X. Zhong, H. Wang, J. Zhang, H. Liu, S. Zhang, H. F. Song, G. Yang, L. Zhang, and Y. Ma, *Tellurium Hydrides at High Pressures: High-Temperature Superconductors*, Phys Rev Lett **116**, 057002, (2016).
- [25] W. Chen, D. V. Semenov, A. G. Kvashnin, X. Huang, I. A. Kruglov, M. Galasso, H. Song, D. Duan, A. F. Goncharov, V. B. Prakapenka, A. R. Oganov, and T. Cui, *Synthesis of molecular metallic barium superhydride: pseudocubic BaH₁₂*, Nat Commun **12**, 273, (2021).
- [26] D. V. Semenov, W. Chen, X. Huang, D. Zhou, I. A. Kruglov, A. B. Mazitov, M. Galasso, C. Tantardini, X. Gonze, A. G. Kvashnin, A. R. Oganov, and T. Cui, *Sr-Doped Superionic Hydrogen Glass: Synthesis and Properties of SrH₂₂*, Adv Mater **34**, e2200924, (2022).
- [27] C. L. Zhang, X. He, Z. W. Li, S. J. Zhang, B. S. Min, J. Zhang, K. Lu, J. F. Zhao, L. C. Shi, Y. Peng, X. C. Wang, S. M. Feng, R. C. Yu, L. H. Wang, V. B. Prakapenka, S. Chariton, H. Z. Liu, and C. Q. Jin, *Superconductivity above 80 K in polyhydrides of hafnium*, Materials Today Physics **27**, (2022).
- [28] F. Hong, P. F. Shan, L. X. Yang, B. B. Yue, P. T. Yang, Z. Y. Liu, J. P. Sun, J. H. Dai, H. Yu, Y. Y. Yin, X. H. Yu, J. G. Cheng, and Z. X. Zhao, *Possible superconductivity at ~70 K in tin hydride SnH_x under high pressure*, Materials Today Physics **22**, (2022).
- [29] Y. Sun, J. Lv, Y. Xie, H. Liu, and Y. Ma, *Route to a Superconducting Phase above Room Temperature in Electron-Doped Hydride Compounds under High Pressure*, Phys Rev Lett **123**, 097001, (2019).
- [30] F. Peng, Y. Sun, C. J. Pickard, R. J. Needs, Q. Wu, and Y. Ma, *Hydrogen Clathrate Structures in Rare Earth Hydrides at High Pressures: Possible Route to Room-Temperature Superconductivity*, Phys Rev Lett **119**, 107001, (2017).
- [31] M. Du, H. Song, Z. Zhang, D. Duan, and T. Cui, *Room-Temperature Superconductivity in Yb/Lu Substituted Clathrate Hexahydrides under Moderate Pressure*, Research **2022**, 1, (2022).
- [32] Z. Zhang, T. Cui, M. J. Hutcheon, A. M. Shipley, H. Song, M. Du, V. Z. Kresin, D. Duan, C. J. Pickard, and Y. Yao, *Design Principles for High-Temperature Superconductors with a Hydrogen-Based Alloy Backbone at Moderate Pressure*, Phys Rev Lett **128**, 047001, (2022).
- [33] D. Duan, Y. Liu, F. Tian, D. Li, X. Huang, Z. Zhao, H. Yu, B. Liu, W. Tian, and T. Cui, *Pressure-induced metallization of dense (H₂S)₂(H₂) with high-T_c superconductivity*, Sci Rep **4**, 6968, (2014).
- [34] D. F. Duan, X. L. Huang, F. B. Tian, D. Li, H. Y. Yu, Y. X. Liu, Y. B. Ma, B. B. Liu, and T. Cui, *Pressure-induced decomposition of solid hydrogen sulfide*, Physical Review B **91**, 180502(R), (2015).

- [35] H. Liu, Naumov, II, R. Hoffmann, N. W. Ashcroft, and R. J. Hemley, *Potential high-Tc superconducting lanthanum and yttrium hydrides at high pressure*, Proc Natl Acad Sci U S A **114**, 6990, (2017).
- [36] F. Hong, L. Yang, P. Shan, P. Yang, Z. Liu, J. Sun, Y. Yin, X. Yu, J. Cheng, and Z. Zhao, *Superconductivity of Lanthanum Superhydride Investigated Using the Standard Four-Probe Configuration under High Pressures*, Chinese Physics Letters **37**, (2020).
- [37] H. Xie, Y. Yao, X. Feng, D. Duan, H. Song, Z. Zhang, S. Jiang, S. A. T. Redfern, V. Z. Kresin, C. J. Pickard, and T. Cui, *Hydrogen Pentagraphenelike Structure Stabilized by Hafnium: A High-Temperature Conventional Superconductor*, Phys Rev Lett **125**, 217001, (2020).
- [38] D. V. Semenov, I. A. Kruglov, I. A. Savkin, A. G. Kvashnin, and A. R. Oganov, *On Distribution of Superconductivity in Metal Hydrides*, Current Opinion in Solid State and Materials Science **24**, 100808, (2020).
- [39] C. J. Pickard and R. J. Needs, *Ab initio random structure searching*, J Phys Condens Matter **23**, 053201, (2011).
- [40] D. C. Lonie, J. Hooper, B. Altintas, and E. Zurek, *Metallization of magnesium polyhydrides under pressure*, Physical Review B **87**, (2013).
- [41] X. Ye, N. Zarifi, E. Zurek, R. Hoffmann, and N. W. Ashcroft, *High Hydrides of Scandium under Pressure: Potential Superconductors*, The Journal of Physical Chemistry C **122**, 6298, (2018).
- [42] A. M. Shipley, M. J. Hutcheon, R. J. Needs, and C. J. Pickard, *High-throughput discovery of high-temperature conventional superconductors*, Physical Review B **104**, (2021).
- [43] N. P. Salke, M. M. Davari Esfahani, Y. Zhang, I. A. Kruglov, J. Zhou, Y. Wang, E. Greenberg, V. B. Prakapenka, J. Liu, A. R. Oganov, and J. F. Lin, *Synthesis of clathrate cerium superhydride CeH₉ at 80-100 GPa with atomic hydrogen sublattice*, Nat Commun **10**, 4453, (2019).
- [44] W. Chen, D. V. Semenov, X. Huang, H. Shu, X. Li, D. Duan, T. Cui, and A. R. Oganov, *High-Temperature Superconducting Phases in Cerium Superhydride with a Tc up to 115 K below a Pressure of 1 Megabar*, Physical Review Letters **127**, 117001, (2021).
- [45] Y. Song, J. Bi, Y. Nakamoto, K. Shimizu, H. Liu, B. Zou, G. Liu, H. Wang, and Y. Ma, *Stoichiometric Ternary Superhydride LaBeH₈ as a New Template for High-Temperature Superconductivity at 110 K under 80 GPa*, Phys Rev Lett **130**, 266001, (2023).
- [46] L. R. Testardi, *Structural instability and superconductivity in A-15 compounds*, Reviews of Modern Physics **47**, 637, (1975).
- [47] K. Abe and N. W. Ashcroft, *Quantum disproportionation: The high hydrides at elevated pressures*, Physical Review B **88**, 174110 (2013).
- [48] Z. J. Shao, D. F. Duan, Y. B. Ma, H. Y. Yu, H. Song, H. Xie, D. Li, F. B. Tian, B. B. Liu, and T. Cui, *Ternary superconducting cophosphorus hydrides stabilized via lithium*, Npj Computational Materials **5**, 1, (2019).
- [49] C. J. Pickard, M. Martinez-Canales, and R. J. Needs, *Density functional theory study of phase IV of solid hydrogen*, Physical Review B **85**, 214114 (2012).
- [50] J. M. McMahon and D. M. Ceperley, *High-temperature superconductivity in atomic metallic hydrogen*, Physical Review B **84**, 144515, (2011).
- [51] I. Errea, F. Belli, L. Monacelli, A. Sanna, T. Koretsune, T. Tadano, R. Bianco, M. Calandra, R. Arita, F. Mauri, and J. A. Flores-Livas, *Quantum crystal structure in the 250-kelvin superconducting lanthanum hydride*, Nature **578**, 66, (2020).
- [52] I. Errea, M. Calandra, C. J. Pickard, J. R. Nelson, R. J. Needs, Y. Li, H. Liu, Y. Zhang, Y. Ma, and

- F. Mauri, *Quantum hydrogen-bond symmetrization in the superconducting hydrogen sulfide system*, Nature **532**, 81, (2016).
- [53] I. Errea, M. Calandra, and F. Mauri, *Anharmonic free energies and phonon dispersions from the stochastic self-consistent harmonic approximation: Application to platinum and palladium hydrides*, Physical Review B **89**, (2014).
- [54] D. V. Semenok, A. G. Kvashnin, A. G. Ivanova, V. Svitlyk, V. Y. Fominski, A. V. Sadakov, O. A. Sobolevskiy, V. M. Pudalov, I. A. Troyan, and A. R. Oganov, *Superconductivity at 161 K in thorium hydride ThH10: Synthesis and properties*, Materials Today **33**, 36, (2020).
- [55] D. V. Semenok, I. A. Troyan, A. G. Ivanova, A. G. Kvashnin, I. A. Kruglov, M. Hanfland, A. V. Sadakov, O. A. Sobolevskiy, K. S. Pervakov, I. S. Lyubutin, K. V. Glazyrin, N. Giordano, D. N. Karimov, A. L. Vasiliev, R. Akashi, V. M. Pudalov, and A. R. Oganov, *Superconductivity at 253 K in lanthanum–yttrium ternary hydrides*, Materials Today **48**, 18, (2021).
- [56] J. Bi, Y. Nakamoto, P. Zhang, Y. Wang, L. Ma, Y. Wang, B. Zou, K. Shimizu, H. Liu, M. Zhou, H. Wang, G. Liu, and Y. Ma, *Stabilization of superconductive La–Y alloy superhydride with T_c above 90 K at megabar pressure*, Materials Today Physics **28**, (2022).
- [57] J. Bi, Y. Nakamoto, P. Zhang, K. Shimizu, B. Zou, H. Liu, M. Zhou, G. Liu, H. Wang, and Y. Ma, *Giant enhancement of superconducting critical temperature in substitutional alloy (La,Ce)H9*, Nat Commun **13**, 5952, (2022).
- [58] W. Chen, X. Huang, D. V. Semenok, S. Chen, D. Zhou, K. Zhang, A. R. Oganov, and T. Cui, *Enhancement of superconducting properties in the La-Ce-H system at moderate pressures*, Nat Commun **14**, 2660, (2023).
- [59] C. Zhang, X. He, Z. Li, S. Zhang, S. Feng, X. Wang, R. Yu, and C. Jin, *Superconductivity in zirconium polyhydrides with $T(c)$ above 70 K*, Sci Bull (Beijing) **67**, 907, (2022).
- [60] X. H. K. Lu, C.L. Zhang, Z.W. Li, S.J. Zhang, B. S. Min, J. Zhang, J.F. Zhao, L.C. Shi, Y. Peng, S.M. Feng, Q.Q. Liu, J. Song, R.C. Yu, X.C. Wang, Y. Wang, M. Bykov, C. Q. Jin, *Superconductivity with T_c 116K discovered in antimony polyhydrides*, arXiv:2310.04033, (2023).
- [61] P. Cudazzo, G. Profeta, A. Sanna, A. Floris, A. Continenza, S. Massidda, and E. K. U. Gross, *Ab initio description of high-temperature superconductivity in dense molecular hydrogen*, Phys Rev Lett **100**, 257001, (2008).
- [62] T. Ma, Z. Zhang, M. Du, Z. Huo, W. Chen, F. Tian, D. Duan, and T. Cui, *High-throughput calculation for superconductivity of sodalite-like clathrate ternary hydrides MXH12 at high pressure*, Materials Today Physics **38**, (2023).